A&A 367, 557–565 (2001)
DOI: 10.1051/0004-6361:20000463

Astronomy & Astrophysics

A census of AGB stars in Local Group galaxies*

I. Photometry of a field in M 31

W. Nowotny[1], F. Kerschbaum[1,3], H. E. Schwarz[2], and H. Olofsson[3]

[1] Institut für Astronomie der Universität Wien, Türkenschanzstraße 17, 1180 Wien, Austria
[2] Nordic Optical Telescope, Apartado 474, 38700 Sta Cruz de La Palma, Canarias, Spain
[3] Stockholms Observatorium, 13336 Saltsjöbaden, Sweden

Received 23 August 2000 / Accepted 5 December 2000

Abstract. We present four colour CCD photometry of a field in M 31. Observations were carried out in two broad band filters (V and i) and two special narrow band "Wing" filters centered on a TiO and a CN molecular band. Colour-magnitude diagrams constructed from broad band photometry show the sequence of RGB/AGB stars. Three known Cepheid variables could be identified on our frames. We used colour-colour diagrams to identify the M- and C-type AGB stars and to investigate e.g. the luminosity function of the AGB population. We found 61 new extragalactic C-stars in this field of M 31.

Key words. stars: asymptotic giant branch (AGB) – stars: carbon – galaxies: individual: M 31 – galaxies: stellar content – techniques: photometric – surveys

1. Introduction

The Asymptotic Giant Branch (AGB) is a relatively short lived (e.g. Vassiliadis & Wood 1993), but decisive phase during the final evolutionary stages for stars with low to intermediate masses (≈0.8–8 $M_\odot$). The vast majority of all stars, which leave the main sequence within a Hubble time, experience it after core helium-burning has ceased, and they appear as late-type giants in the Hertzsprung-Russell diagram (HRD).

The AGB phase is characterized by several important phenomena:
(i) The onset of repeated, explosive helium-burning in a shell [He-shell flashes, or thermal pulses (TP)] accompanied by deep convection, which leads to the production and dredge-up of carbon and heavy elements produced for instance by the s-process (e.g. Iben & Renzini 1983).
(ii) Pulsations with long periods (due to the enormous size and low density of AGB stars), usually combined with large size variations and the formation of shock fronts in the stellar atmosphere (e.g. Willson 1988). Depending on their pulsational properties, these objects are classified as Miras, semi-regular or irregular variables.
(iii) Finally, the development of strong stellar winds (with typical mass loss rates between 10^{-8} and 10^{-4} $M_\odot\,\mathrm{yr}^{-1}$), which will eventually lead to a drastic change in stellar mass. This also produces a cool circumstellar envelope, where complex molecules and dust can form (Habing 1996).

Both their intrinsically high luminosity (with spectral energy distributions peaking in the red or infrared) and their well defined evolutionary stage make them important constituents and probes of extragalactic systems. Because of their high luminosity (up to a few 10^4 $L_\odot$) AGB stars play an important role in studies of stellar populations (Lançon 1999). Due to their age they define highly relaxed subsystems of galaxies and are therefore interesting for work on galactic structure (Dejonghe & Caelenberg 1999). Finally, their mass loss significantly contributes to the enrichment of the interstellar medium (Habing 1996). Traditionally our knowledge of stellar populations in Local Group galaxies comes mainly from photometry of evolved giants. Even in the Large Magellanic Cloud (LMC) the observation of the main sequence is difficult due to crowding and confusion. Recent impressive observations (HST and ground-based) of Local Group galaxies complement our knowledge of other parts of the HRD (see e.g. Aparicio 1999). AGB stars represent important constituents of the intermediate age (1–10 Gyr) stellar population in external galaxies and allow us to probe the star formation history for this time interval (Grebel 1999). AGB stars can be

Send offprint requests to: W. Nowotny,
e-mail: nowotny@astro.univie.ac.at

* Based on observations made with the Nordic Optical Telescope operated on the island of La Palma jointly by Denmark, Finland, Iceland, Norway, and Sweden, in the Spanish Observatorio del Roque de los Muchachos of the Instituto de Astrofisica de Canarias.

useful as distance estimators, too. Not only the relatively well defined period-luminosity (PL) relation of Mira variables, but also the narrow luminosity function of carbon stars can be used for this purpose.

On the other hand, extragalactic studies are important for our understanding of stellar evolution on the AGB itself (Zijlstra 1999). Extragalactic systems with their often well defined distances, metallicities, and star formation histories provide important tests for theoretical models by limiting the parameter space. Starting with an oxygen-rich (C/O < 1) atmosphere at the onset of the AGB evolution, stars within the mass range of $\approx$1.5–4 $M_{\odot}$ can become carbon-rich (C/O > 1) during the TP-AGB phase, i.e. the spectral type changes from M to S (C/O ≈ 1) and finally to C. Among the most interesting AGB problems addressable by extragalactic research is the formation of these carbon-stars (e.g. the lower and upper mass limit). Another very important problem is the dependence of mass loss on mass, metallicity, and evolutionary age. By observing populations of different metallicity some light can be shed on these and other questions.

In general, large samples of AGB stars are needed for most investigations of their general properties (e.g. for a distance estimation from the C-star luminosity function). However, typically less than 10 C-stars are known in each of even the nearest satellite galaxies (see e.g. Groenewegen 1999, and references therein). In M 31 (the Andromeda galaxy) fewer than 250 C-stars have been identified, whereas some 10^4 are expected from a comparison with the LMC (Brewer et al. 1995). Only the LMC, the SMC, and the Fornax dwarf galaxy can be called "well studied" in this respect (e.g. Azzopardi 1999; Cioni et al. 2000).

Therefore, the efficient detection and characterization of such objects in extragalactic systems is essential for all the above mentioned studies.

2. The method

Different methods have been used to find extragalactic AGB stars (e.g. Richer 1989; Groenewegen 1999): (i) low dispersion objective prism observations (Westerlund 1978); (ii) optical follow-up spectroscopy on stars identified in colour-magnitude diagrams (Cannon et al. 1981; Aaronson & Mould 1980); (iii) grism surveys (Westerlund 1979); and finally (iv) narrow band photometry, described in more detail below. While (i) and (iii) are normally impossible in crowded regions, (ii) is a perfect follow-up method, but with few exceptions inefficient or not feasible in larger systems (often a few 10^3 interesting objects). Since photometry in crowded regions is still possible, method (iv) turns out to be quite powerful and plays an important part for statistical studies and the pre-selection for spectroscopic follow-up programmes in external galaxies.

Wing & Stock (1973) first proposed, that a subset of the eight-filter system of Wing (1971) could be very useful in a search for and chemical characterization of AGB stars, and it has proven to be quite successful. A description can be found e.g. in Palmer & Wing (1982) or Cook & Aaronson (1989). Later the method was developed and refined for CCD use by two groups (led by H. Richer and M. Aaronson). It uses conventional V and I filters as temperature indicators, whereas two narrow band Wing-filters around 800 nm provide low-resolution spectral information for discriminating between O- and C-rich stars.

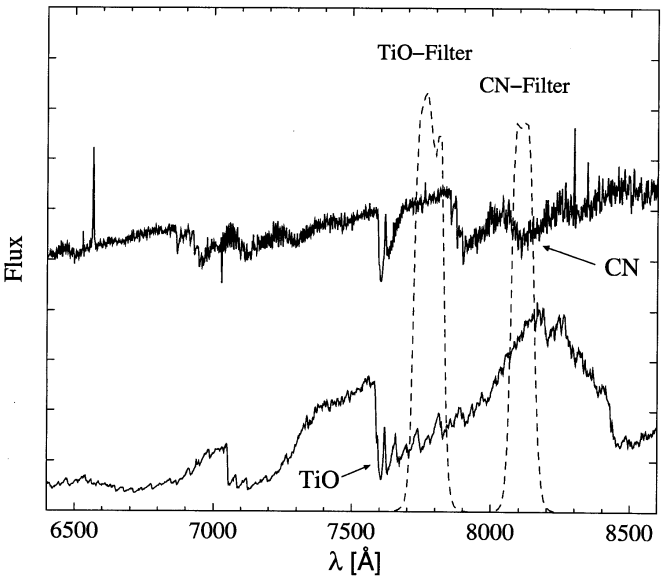

Fig. 1. Transmission curves of the two narrow band filters, and typical spectra (Schultheis 1998) of a C3.2 III (upper) and a M6.3 III star (lower)

Figure 1 shows the filter curves of the narrow band filters (we bought, to start our search for AGB stars in Local Group galaxies), together with typical AGB star spectra demonstrating the principle of the selection method. The first filter is centered on a TiO band, which is prominent in M-stars and on a relatively clean piece of "continuum" in C-stars, while the second one is centered on a CN band, which is prominent in C-stars and on the "continuum" in M-stars. This gives a strong contrast between the measures taken in these two filters, and the colour index (TiO−CN) can efficiently separate the two spectral types.

The synthetic colours in Fig. 2 are calculated by folding the measured response curves of our new narrow band filters with the CCD[1] QE curve (taken from the NOT webdocumentation) and spectroscopic data from the literature: synthetic M-giant spectra from Fluks et al. (1994), synthetic hydrostatic C-star spectra from Loidl (priv. communication; C11026 e.g. means C-star with C/O = 1.1 and $T_{\rm eff} = 2600$ K), and the remaining from the spectrophotometric atlas of Pickles (1998). While the features of TiO/CN do not have significant strengths for stars bluer than $(V-i) \approx 1.5^{\rm mag}$ [and therefore (TiO−CN) $\approx 0^{\rm mag}$],

[1] See Sect. 3.1.

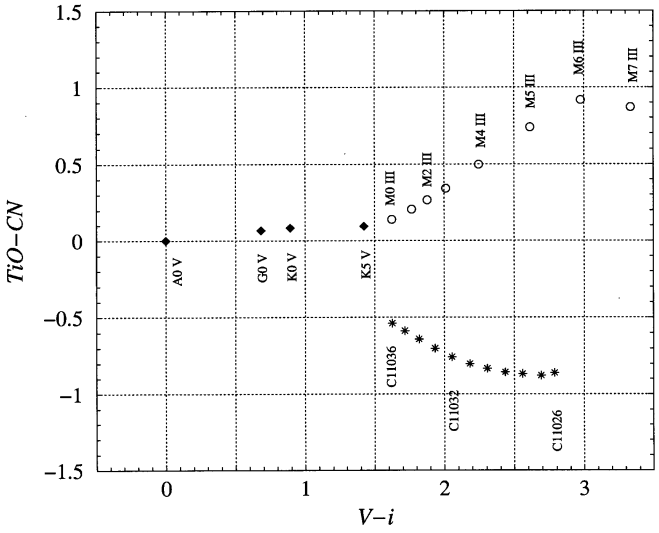

Fig. 2. Colour-colour diagram with synthetic colours for different spectral types and chemistries. Early stars have no TiO/CN-features, but late-type stars can be clearly separated into O- and C-rich by photometric means

they become prominent for later stars. Their strengths increase strongly with the spectral type, and so does the colour index (TiO−CN). In the colour-colour diagram (Fig. 2) a clear bifurcation between M- and C-stars can be seen towards the red end of the sequence. It can be used to identify and characterize them.

This method works well, as was already shown e.g. by Brewer et al. (1995, 1996). We plan to use it to investigate the AGB populations of Local Group galaxies.

3. Data

3.1. Observations

Our observations were carried out with the Nordic Optical Telescope (NOT), La Palma, using the ALFOSC focal reducer instrument with the Loral-Lesser (2048×2048) CCD during the two nights of September 29 and 30, 1998 (see `www.not.iac.es` for details). The basic instrumental data are listed in Table 1. As broad band filters we used Bessell V and Gunn i, the filter properties are listed in Table 2.

Brewer et al. (1995) observed 5 fields in M 31 with the above described method. The larger the samples of known AGB stars are, the more reliable are the derived properties of this population. As this work covered only about 2% of the whole M 31-area, we selected an additional field in M 31 for a first test of our new filter set centered on $\alpha_{2000} = 0^{\rm h}39^{\rm m}53^{\rm s}$ and $\delta_{2000} = 40°25'28''$ (also aiming for a comparison of our results with the comprehensive work of Brewer et al. 1995). This test field is located between their fields 3 and 4, about 14 kpc south-west of the centre of M 31 along its major axis. Table 3 summarizes our observations of the field in M 31 and the calibration observations in the Selected Area fields #110 and #95, for which we used V and i data from Landolt (1992). Both nights were photometric, and the seeing varied between $1''$ and $1\farcs3$ on the combined frames.

Table 1. Instrumental data of NOT/ALFOSC

Main mirror diameter	2.56 m
CCD size	2048×2048 pixels
Field of view	$6\farcm5 \times 6\farcm5$
Pixel size	15 μm
Pixel scale	$0\farcs189$/pixel
Readout noise	6.6 e^-
Gain	1.07 e^-/ADU

Table 2. The filters used

Filter	NOT #	λ_c (Å)	$\Delta\lambda$ (Å)	System
V	75	5300	800	Bessell
i	12	7970	1570	Gunn
TiO	–	7780	110	Wing
CN	–	8113	85	Wing

Table 3. Observing log

Field	Filter	Exp.time	Field	Filter	Exp.time
M 31	V	3 × 400 s	SA110	V	30 s
	i	3 × 400 s		i	10 s
	TiO	4 × 1200 s		TiO	130 s
	CN	4 × 1200 s		CN	250 s
			SA95	V	35 s
				i	20 s
				TiO	180 s
				CN	240 s

3.2. Reduction and calibration

The basic reduction of all frames was done with MIDAS (bias and dark subtraction, flat-fielding, cosmic ray removal, summing, and cropping). The narrow band filters were used in the converging beam of the telescope to avoid wavelength shifts due to the large angles of incidence in parallel beam instruments such as ALFOSC. This resulted in some vignetting and all frames were cropped to 1700 × 1600 pix^2 or $5\farcm3 \times 5'$, in order to use only the unvignetted area. Photometry on the combined frames was done with the PSF-photometry reduction packages DAOPHOT II and ALLSTAR within MIDAS (Stetson 1987, *DAOPHOT User's Manual).* After a detailed analysis of the influence of DAOPHOT/ALLSTAR parameters we have chosen the following quality criteria for stars to be considered in the further analysis: *sharp* was allowed to range between −5 and 5; the formal magnitude error (error of PSF-fitting) was allowed to reach $\sigma < 0.1^{\rm mag}$

Table 4. Observed Cepheids in the field

#	Period [d]	Filter	app. mag calc.	app. mag obs.
168	13.125	V_0	19.9	19.2
		i_0	19.1	18.8
(192)	(4.773)	V_0	(21.1)	(20.1)
		i_0	(20.5)	(19.5)
193	15.524	V_0	19.7	19.0
		i_0	18.9	18.5

for i_0, $(V-i)_0$, and $(\mathrm{TiO}-\mathrm{CN})_0$ (see below for further information on the selection criteria).

The standard fields SA95 and SA110 of Landolt (1992) were observed to obtain the photometric zeropoints for the V and i filters. The similarity of Landolt's Cousins i-filter ($\lambda_c = 7900$ Å and $\Delta\lambda = 1500$ Å) and our i-filter (see Table 2) motivated this approach.

No photometric calibration was done for the two narrow band filters. As we know, that stars with "early" spectral type lack TiO/CN-features, and therefore have $(\mathrm{TiO}-\mathrm{CN})_0 \approx 0^{\mathrm{mag}}$, we can use them as a photometric calibration for this colour index. Choosing "blue" stars $[(V-i)_0 < 0.7^{\mathrm{mag}}]$, with strict quality criteria ($\sigma < 0.05^{\mathrm{mag}}$ for all filters and colour indices, *sharp* between -1.5 and 1.5) we determined an offset in $(\mathrm{TiO}-\mathrm{CN})_0$ of 0.37^{mag}, which we applied to all stars.

For the atmospheric extinction correction the standard coefficients for KPNO of $k_V = 0.152$, $k_i = 0.061$, $k_{\mathrm{TiO}} = 0.055$ and $k_{\mathrm{CN}} = 0.051$ were applied.

As a check of the reliability of our photometry we tried to identify known Cepheids in our field, which lies just on the south-western border of field III in Baade & Swope (1965). It turned out, that we have variables #168, #192, and #193 in common. These are Cepheids with periods of 13.125, 4.773, and 15.524 days, respectively. By using the mean PL-relationships given in Groenewegen & Oudmaijer (2000), a distance modulus for M 31 of $(m-M) = 24.43^{\mathrm{mag}}$ (Freedman & Madore 1990), and applying the reddening corrections given below to our observations, we get the results listed in Table 4. The photometry of star #192 is affected by a nearby field star, and the results are therefore only listed for reference.

Keeping in mind the random Cepheid phases of our observations, the known m_{phot}-amplitudes of the Cepheids (1.3^{mag}, 0.7^{mag}, and 1.55^{mag}, respectively), the low number of Cepheids found, as well as the accuracy of our photometry (typically around 0.08^{mag} in V and 0.13^{mag} in i), the measured and calculated values are consistent. The shift of V_0 and i_0 into the same direction suggests to be caused by pulsation, i.e. a change in luminosity. Moreover, one should note that the determination of the interstellar reddening E_{B-V} contributes an additional uncertainty (see below). For a more definite statement a larger sample of Cepheids is needed. The positions of the identified Cepheids in the colour-magnitude diagram (CMD) can be seen in Fig. 5.

3.3. Interstellar reddening

The correction for interstellar reddening was done following the method described by Brewer et al. (1995). A foreground reddening E_{B-V} of 0.23^{mag} was assumed, leading to an absorption of $A_V = 3.1 \cdot 0.23 = 0.713^{\mathrm{mag}}$ and $A_i = 0.6 \cdot A_V = 0.428^{\mathrm{mag}}$. No correction was made for the TiO and CN data because of a negligible difference in center wavelength between the two filters and our artificial zeroing of the (TiO−CN) colour index.

A note on the reliability of this approach. Within our field (having a size of ≈1.1 kpc at the distance of M 31) the amount of internal extinction will definitely vary (our V frame shows clear indications of dark clouds). Moreover we will find objects at different "depths" in the disk. This will lead to an additional uncertainty in our $(V-i)$ colour indices, acting as the temperature indicator. But it will *not* affect the (TiO−CN) values due to the very small difference in the center wavelengths of the Wing filters [using the calculations of Battinelli & Demers (2000) we find, that $E_{\mathrm{TiO-CN}}$ is negligible]. To get a feeling for this influence, we plotted a 1 kpc-reddening-vector with rough absorption values, known from the Milky Way ($A_V = 1^{\mathrm{mag}}$, $A_I = 0.43^{\mathrm{mag}}$, $E_{V-I} = 0.57^{\mathrm{mag}}$), in the diagrams. This uncertainty may affect some quantitative measurements, such as the star counts in the selection areas, the mean magnitudes of the luminosity functions (LF), and hence the distance determinations derived from the C-star LF.

3.4. Astrometry

The astrometric calibration within our field was done in two steps. First, all individual filter results were paired using the DENIS-software "Cross_Color" with the i filter as reference. A pairing-radius of 3 pixel, corresponding to ≈0.″6, was chosen after testing a range of values. This procedure led to a total of 5448 stars having V and i measurements (*sample 1*) out of which 2546 stars also have the corresponding TiO and CN data (*sample 2*).

As a second step, an astrometric solution was produced for all stars, using the *ASTROMET*–package of MIDAS and four field stars included in the Guide Star Catalogue (2788_1818, 2788_1555, 2788_1453, –2_627), which were on our frames. A list of coordinates and photometric results of the C stars identified in Sects. 4.2 and 4.5 can be found in Table A1. Typical accuracies of the photometry are $\sigma_I = 0.02^{\mathrm{mag}}$, $\sigma_{V-I} = 0.06^{\mathrm{mag}}$, $\sigma_{A-B} = 0.04^{\mathrm{mag}}$.

3.5. Detectability

From the total number of objects detected in each of the filters it is clear, that the combined i frame is the deepest exposure. In both, the narrow band filters (TiO and CN) and V, we have not reached a sufficient limiting magnitude

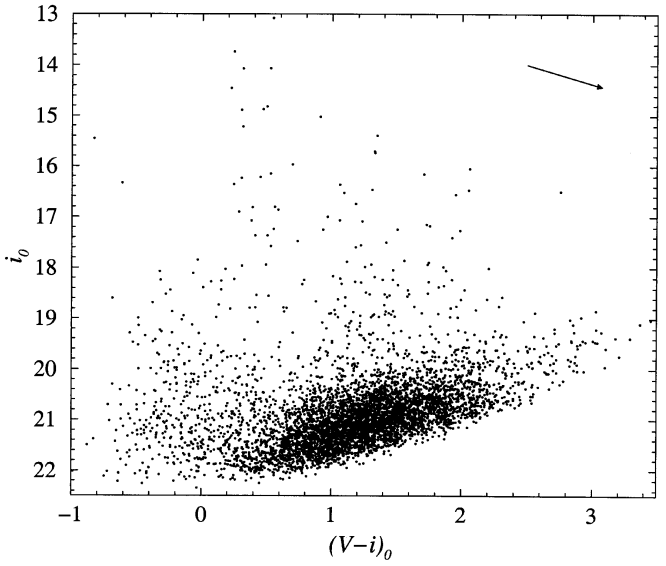

Fig. 3. Colour-magnitude diagram for all stars of *sample 1*. Also plotted is a 1 kpc-reddening-vector for absorption within the disc of M 31 (as described in the text)

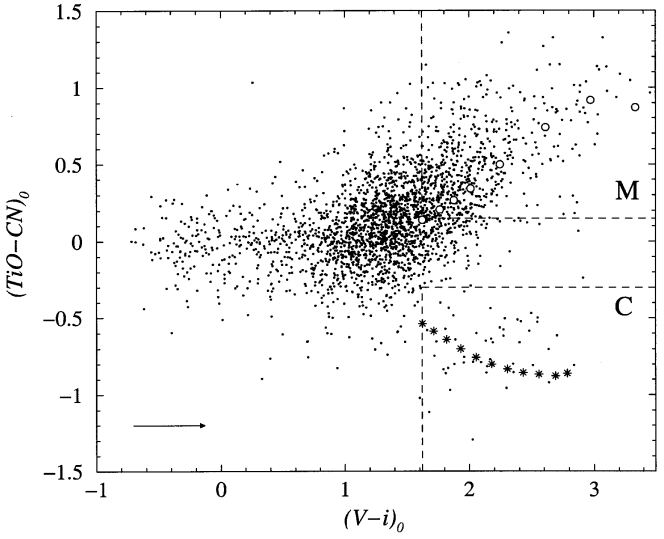

Fig. 4. Colour-colour diagram for the stars of *sample 2*, and the selection areas for M- and C-stars (as described in the text). Synthetic photometry is plotted as well (M-stars with open circles, C-stars with asterisks). Again a 1 kpc-reddening-vector for absorption is plotted (as described in the text)

for certain groups of objects. First, the V exposure is not long enough to reach all red objects, which we detect even in the narrow band filters (see Sect. 4.5). Second, many blue objects were too faint to be detected in TiO and CN. These are the main reasons for the different sizes of *sample 1* and *sample 2*. Since we were not interested in TiO and CN data for the warmer objects, the second limitation is of no relevance for the results in this paper.

4. Results

4.1. Colour-magnitude diagram

Figure 3 shows the CMD for all 5448 stars of *sample 1*, which matched the above mentioned quality criteria. One can see the upper three magnitudes of the sequence of RGB and AGB stars, above this are bright red supergiants (RSG). At $(V-i)_0 \approx 0^{\rm mag}$ one can see a component of relatively blue stars. This arises from the fact, that our field lies "near" a spiral arm of M 31, where star formation takes place. Field 3 of Brewer et al. (1995) lies in the spiral arm and shows an even stronger blue component. Field 5 of this paper gives also an estimate of an upper limit of the galactic foreground contribution, since it lies more than 32 kpc from the center of M 31. It turns out, that the foreground contributes nothing for $(V-i)_0$ bluer than about 1.

4.2. Colour-colour diagram

For the 2546 stars of *sample 2*, which matched our quality criteria, a colour-colour diagram (CCD) is drawn in Fig. 4. The bifurcation of $\approx 1^{\rm mag}$ on the righthand side, due to the separation of the M- and C-stars, is obvious. Photometric variability and a varying amount of M 31 internal reddening could contribute to the scatter of these two sequences.

We defined the selection criteria for M/C-stars as follows: The border in $(V-i)_0$ was chosen in accordance with our synthetic photometry (see Fig. 2). We determined a scatter for all early stars $[(V-i)_0 < 0.7^{\rm mag}]$ in $({\rm TiO}-{\rm CN})_0$ with $\sigma = 0.2^{\rm mag}$. The criteria for $({\rm TiO}-{\rm CN})_0$ were then chosen in order to separate the areas for M/C-stars by 2.5σ of this scatter. Brewer et al. (1995) confirmed these latter selection criteria with explicit spectroscopic observations.

The following selection criteria for M/C-star candidates were used (and are drawn in the CCD of Fig. 4):

- M: $(V-i)_0 > 1.62^{\rm mag}$, $({\rm TiO}-{\rm CN})_0 > 0.15^{\rm mag}$, $i_0 > 18.5^{\rm mag}$ (no RSGs, galactic contamination), $M_{\rm bol} < -3.5^{\rm mag}$ (tip of the RGB, see Sect. 4.3)
- C: $(V-i)_0 > 1.62^{\rm mag}$, $({\rm TiO}-{\rm CN})_0 < -0.3^{\rm mag}$.

Stars with $(V-i)_0 > 1.62^{\rm mag}$ and $({\rm TiO}-{\rm CN})_0$ between the selection areas could be candidate S-stars (spectroscopically confirmed by Brewer et al. 1996). The criteria must be kept constant for investigations of further fields or galaxies, in order to be consistent in comparing the numbers of selected stars.

Figure 5 shows a CMD for the stars of *sample 2*. The 286 M-stars and 47 C-stars from the selection areas of Fig. 4 are drawn with open circles and asterisks, respectively. They lie on the upper end of the RGB- and the AGB-sequence. Moreover, the identified Cepheids are indicated by filled squares.

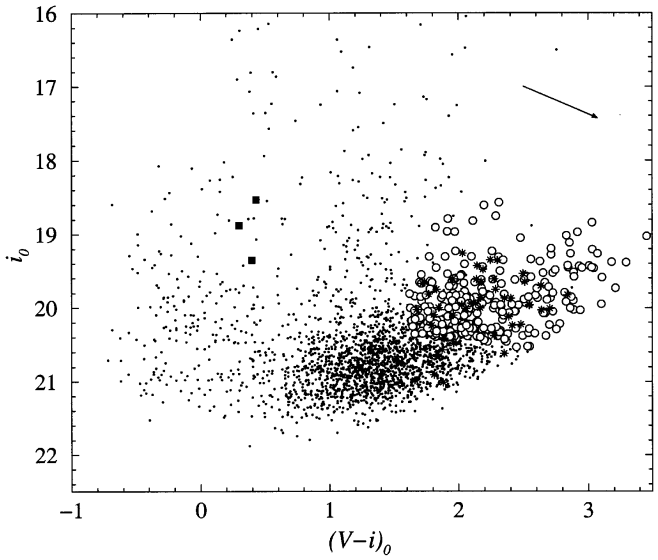

Fig. 5. Colour-magnitude diagram for all stars of *sample 2*. All stars in the selection areas (M-stars with open circles, C-stars with asterisks) and the identified Cepheides (filled squares) are indicated. In the upper right corner the 1 kpc-reddening-vector is plotted (as described in the text)

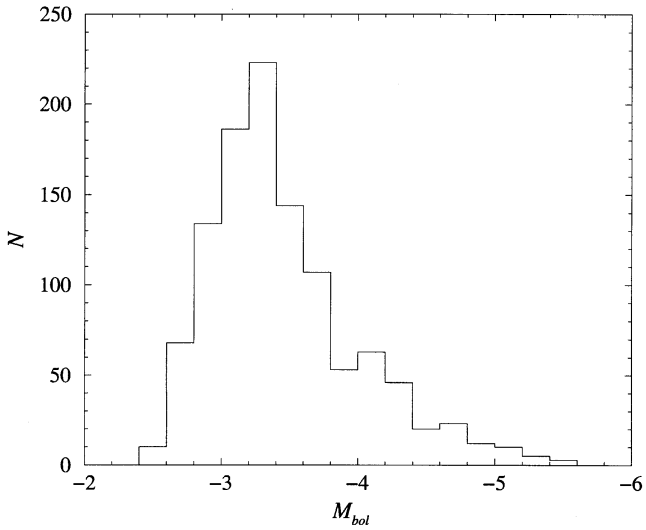

Fig. 6. Bolometric LF for the AGB candidates of *sample 1*, selected as described in the text

4.3. Luminosity function

The bolometric LF is one of the important concepts used for comparing AGB models with observations. It gives clues to many topics (star formation history (SFH), stellar evolution, inital mass function, mass loss rates, ...) and led to the refinement of the AGB theory in the past (e.g. *bright C-star mystery* → different mass loss laws, semi-convection, overshooting, hot bottom burning, ...).

To compare our results with those of Brewer et al. (1995), we calculated a bolometric LF for the AGB star candidates of *sample 1*, which were selected using the following criteria:

- $(V-i)_0 > 1.62^{\rm mag}$
- $i_0 > 18.5^{\rm mag}$
- $-7^{\rm mag} > M_{\rm bol} > -1^{\rm mag}$.

To calculate the absolute bolometric magnitude $M_{\rm bol}$ of late-type stars we used a distance modulus for M 31 of $(m-M) = 24.43^{\rm mag}$ (Freedman & Madore 1990) and the bolometric correction (BC) given by Bessel & Wood (1984):

$$M_{\rm bol} = i_0 + BC - 24.43$$
$$BC = 0.3 + 0.38 \cdot (V-i_{\rm C})_0 - 0.14 \cdot (V-i_{\rm C})_0^2.$$

This Cousins-system BC is valid for M-stars, which have $1 < (V-I) < 6$. It was – in accordance with Brewer et al. (1995) – used for C-stars too, although it is not fully correct in this case. We can use this Cousins-i relation, because our Gunn-i observations are calibrated to the Cousins-system (see Sect. 3.2).

By comparing some characteristics of the diagrams (blue component, Cepheids and RSGs in the CMD; number of bright AGB stars and steepness of the LF) of different fields, one can draw conclusions for the SFHs (see e.g. Grebel 1999). Figure 6 shows the bolometric LF for all AGB candidates. A comparison of it with Fig. 9 of Brewer et al. (1995) reveals, that it is very similar to the LFs of their fields 3 and 4, for which active SF is concluded for the last few Gyrs.

Figure 7 shows the i_0-LF of the selected M/C-stars (of Fig. 4), where the histogram of the M-stars is scaled by a factor of 0.1 to simplify the comparison. C-stars have a lower mean i_0-magnitude, which may reflect the fact, that stars can change their spectral type from M to C by the third dredge-up, while they ascend the AGB. The bolometric LF of the C-stars (calculated with a BC, which we derived from data of C-stars in Bessel & Wood 1984) seems to be consistent with the one of Groenewegen (1999).

4.4. C-stars

Taking into account that (due to the short evolutionary stage) optically detectable C-stars have a relatively small scatter in their i-magnitudes, they can be used to estimate the distance of the population. The results of Brewer et al. (1995) showed that neither different star formation histories nor different metallicities strongly influence the mean i-magnitudes of a population of C-stars, which makes them a useful standard candle. The observations of Richer (1981) and Richer et al. (1985) resulted in a mean absolute i-magnitude of $\langle M_I \rangle = -4.75 \pm 0.47^{\rm mag}$ for a sample of LMC C-stars. Combining this with the mean apparent magnitude $\langle m_I \rangle = 19.96 \pm 0.4^{\rm mag}$ of the above selected C-star candidates (Fig. 7) results in a distance modulus of $(m-M) = 24.71 \pm 0.62^{\rm mag}$, which is in agreement with other distance determinations, e.g. the one by Freedman & Madore (1990).

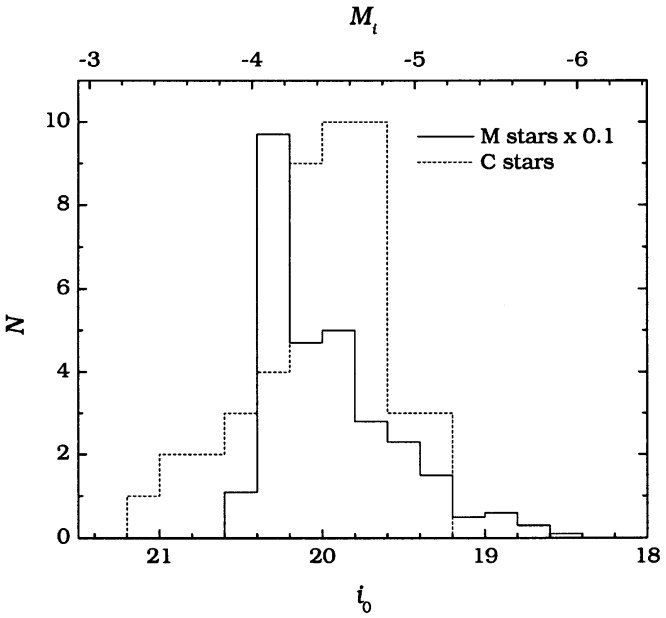

Fig. 7. LFs for the selected M- (286 stars) and C-stars (47); the former was multiplied by a factor of 0.1 to simplify the comparison

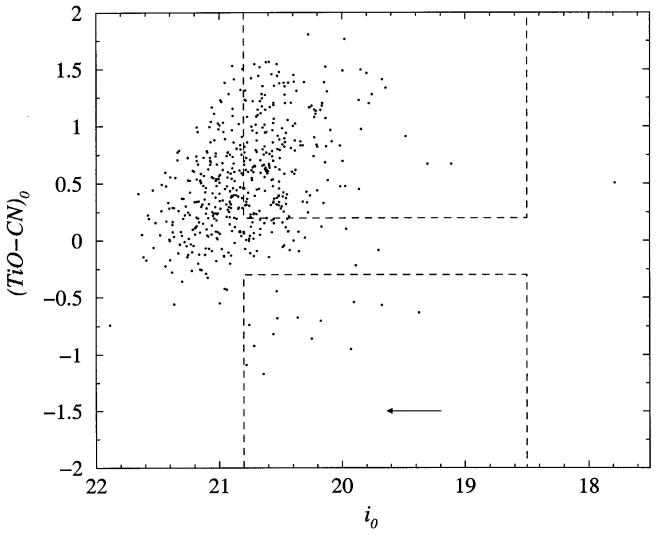

Fig. 8. Diagram to select AGB candidates from stars without V photometry. In the lower right corner the 1 kpc-reddening-vector for absorption within the disc of M 31 is shown

4.5. Stars without V photometry

For our observational test run the exposure time of the V frames was too short. Therefore, we have 515 red stars, which are too weak in the V band to have reliable measurements. However, we can still use photometry in the other three filters to select AGB candidates, as Fig. 8 demonstrates. The lower limit in i can be choosen for example as the magnitude of the tip of the RGB ($i_0 = 20.8^{\rm mag}$, see Brewer et al. 1995), while the upper limit is the magnitude of the end of the RGB/AGB-sequence in the CMD. The borders in $(\mathrm{TiO}-\mathrm{CN})_0$ are the same as for the stars with photometry in all four filters. Doing this, we identify another 14 C- and 221 M-star candidates. This rough selection does not consider variable magnitudes (can be above $1^{\rm mag}$ in i on the AGB), but could be very useful for observations of very distant galaxies, as the observing time for the V-filter can be saved.

With all C/M-stars from the Sects. 4.2 and 4.5, we get a C/M-ratio of ≈0.12. This result is again similar to the "raw" C/M-ratio of the neighbouring field 4 of Brewer et al. (1995).

5. Summary and outlook

As a first test for our new filter set we observed a field in M 31. Plotting colour-colour diagrams of the photometry of the two broad band filters (V and i) and the two narrow band filters (TiO and CN), one can easily separate O- and C-rich AGB stars by photometric means. Besides we showed, that a special "CMD" with i_0 and $(\mathrm{TiO}-\mathrm{CN})_0$ can be used to sort out candidates, even without photometry in the V band. We found 286 (+221) new M- and 47 (+14) new C-star candidates in M 31. We enlargened the sample of known M 31 C-stars by 25%. Our derived properties of the AGB population in the studied M 31-field are consistent with those of Brewer et al. (1995).

A comparison between the results (e.g. star numbers) of all galaxies, which have been investigated so far with this technique by different groups (e.g. Brewer et al. 1995 or Albert et al. 2000), seems interesting. Unfortunately, this is not a "straightforward" task, due to differencies in some details of their work (properties of the narrow band filters, selection criteria, ...).

Our future work will concentrate on other galaxies within the Local Group, where we want to study the AGB population. Observations have already been carried out.

Our observations will also form the basis of follow-up monitoring and spectroscopy. We want to enlarge the often very small samples of known extragalactic AGB stars to statistically meaningful numbers, derive LFs for M- and C-stars, compare the LFs among the different galaxies including the (better known) LFs of the LMC and SMC, and correlate them with their respective star formation histories.

Acknowledgements. This work was supported by APART (Austrian Programme for Advanced Research and Technology) from the Austrian Academy of Sciences, the Österreichische Nationalbank under the Jubiläumsfonds-project number 6876 and the Fonds zur Förderung der wissenschaftlichen Forschung under project number S7308-AST. The authors are very grateful to Rita Loidl, who provided us with synthetic spectra of C-stars. We used the Simbad database operated at CDS, Strasbourg, France.

Appendix A: M 31 carbon stars

Table A1. The C-rich AGB star candidates found in M 31. Coordinates are in (J2000.0). Stars 1–47 are chosen from Fig. 4. Stars 48–61 are chosen from Fig. 8 (without V photometry)

#	RA	DEC	i	$V-i$	TiO−CN	#	RA	DEC	i	$V-i$	TiO−CN
	[h m s]	[° ′ ″]	[mag]	[mag]	[mag]		[h m s]	[° ′ ″]	[mag]	[mag]	[mag]
1	0:39:40.58	40:23:01.2	21.01	1.88	−0.80	31	0:40:00.54	40:25:12.4	19.87	2.36	−0.85
2	0:39:41.23	40:24:07.8	19.61	2.14	−0.86	32	0:40:00.74	40:23:00.3	19.36	2.30	−0.96
3	0:39:41.25	40:22:46.0	20.63	1.84	−0.43	33	0:40:00.75	40:25:29.8	19.66	1.74	−0.65
4	0:39:41.83	40:24:34.0	20.24	2.41	−0.52	34	0:40:02.44	40:22:48.2	20.10	1.81	−0.57
5	0:39:42.70	40:25:40.2	19.43	2.14	−0.81	35	0:40:02.76	40:23:41.6	19.26	2.03	−0.79
6	0:39:44.70	40:26:36.1	20.24	1.79	−0.84	36	0:40:03.35	40:24:03.7	19.48	2.19	−0.66
7	0:39:44.81	40:24:55.4	19.35	2.24	−0.56	37	0:40:03.61	40:23:16.9	19.75	1.83	−0.83
8	0:39:44.92	40:23:50.1	20.00	1.85	−0.97	38	0:40:03.94	40:27:30.2	20.02	2.06	−0.60
9	0:39:44.96	40:22:56.5	19.61	2.27	−0.62	39	0:40:04.62	40:23:34.2	19.83	2.84	−0.81
10	0:39:45.67	40:22:53.4	20.01	2.17	−0.77	40	0:40:05.30	40:23:47.8	20.57	1.87	−0.49
11	0:39:46.83	40:26:03.0	20.62	2.35	−0.80	41	0:40:05.54	40:25:14.6	20.99	1.66	−0.58
12	0:39:48.27	40:23:54.0	20.49	1.96	−0.33	42	0:40:05.96	40:23:26.4	20.12	2.39	−0.51
13	0:39:48.41	40:24:35.6	20.03	1.68	−1.11	43	0:40:06.11	40:26:08.3	19.87	2.40	−0.66
14	0:39:48.58	40:25:32.1	19.87	2.17	−0.44	44	0:40:06.35	40:25:54.4	20.91	1.81	−0.86
15	0:39:49.89	40:26:20.5	19.65	2.17	−0.64	45	0:40:06.59	40:27:11.2	19.97	2.55	−0.53
16	0:39:50.92	40:24:35.8	19.75	2.29	−0.50	46	0:40:07.26	40:26:07.5	19.94	2.13	−0.65
17	0:39:51.62	40:26:02.5	20.23	2.48	−0.58	47	0:40:07.48	40:26:06.2	19.65	2.51	−0.81
18	0:39:51.64	40:24:20.7	19.61	1.96	−0.79	48	0:39:40.01	40:26:17.0	20.25	–	−0.86
19	0:39:53.04	40:25:16.3	19.67	1.72	−0.75	49	0:39:40.23	40:23:11.8	19.90	–	−0.54
20	0:39:53.26	40:24:14.9	20.38	2.28	−0.58	50	0:39:42.60	40:25:51.5	20.56	–	−0.82
21	0:39:53.61	40:27:07.4	20.01	2.70	−0.62	51	0:39:42.93	40:23:40.8	20.53	–	−0.68
22	0:39:53.75	40:24:41.7	20.04	2.64	−0.92	52	0:39:43.66	40:26:18.1	20.72	–	−0.92
23	0:39:53.90	40:24:59.5	19.94	2.10	−0.79	53	0:39:44.92	40:26:39.9	20.36	–	−0.68
24	0:39:56.55	40:23:50.9	19.54	2.50	−0.47	54	0:39:45.65	40:25:45.3	20.76	–	−0.74
25	0:39:56.84	40:25:42.4	20.42	1.89	−0.64	55	0:39:46.10	40:25:52.3	20.17	–	−0.70
26	0:39:57.67	40:26:44.4	19.96	2.55	−0.50	56	0:39:51.63	40:26:20.9	20.53	–	−0.44
27	0:39:59.41	40:25:52.4	19.82	1.77	−0.40	57	0:39:51.91	40:25:06.0	19.67	–	−0.57
28	0:40:00.10	40:25:14.7	19.97	2.03	−1.29	58	0:39:54.40	40:27:36.5	19.37	–	−0.63
29	0:40:00.11	40:22:40.9	19.70	2.63	−0.70	59	0:39:59.04	40:24:58.2	20.64	–	−1.17
30	0:40:00.31	40:24:57.2	20.10	1.96	−0.75	60	0:40:02.80	40:23:51.1	20.78	–	−1.09
						61	0:40:04.05	40:22:52.0	19.93	–	−0.95

References

Albert, L., Demers, S., & Kunkel, W. E. 2000, AJ, 119, 2780

Aaronson, M., & Mould, J. 1980, ApJ, 240, 804

Aparicio, A. 1999, in The Stellar Content of Local Group Galaxies, ed. P. Whitelock, & R. Cannon, IAU Symp., 192, 304

Azzopardi, M., Muratorio, G., Breysacher, J., & Westerlund, B. E. 1999, in The Stellar Content of Local Group Galaxies, ed. P. Whitelock, & R. Cannon, IAU Symp., 192, 144

Baade, W., & Swope, H. H. 1965, AJ, 70, 212

Battinelli, P., & Demers, S. 2000, AJ, 120, 1801

Bessel, M. S., & Wood, P. R. 1984, PASP, 96, 247

Brewer, J. P., Richer, H. B., & Crabtree, D. R. 1995, AJ, 109, 2480

Brewer, J. P., Richer, H. B., & Crabtree, D. R. 1996, AJ, 112, 491

Cannon, R. D., Niss, B., & Nørgaard-Nielsen, H. U. 1981, MNRAS, 196, 1P

Cioni, M.-R. L., Habing, H. J., & Israel, F. P. 2000, A&A, 358, 9L

Cook, K. H., & Aaronson, M. 1989, AJ, 97, 923

Dejonghe, H., & Van Caelenberg, K. 1999, in Asymptotic Giant Branch Stars, ed. T. Le Bertre, A. Lebre, & C. Waelkens, IAU Symp., 191, 501

Fluks, M. A., Plez, B., Thé, P. S., et al. 1994, A&AS, 105, 311

Freedman, W. L., & Madore, B. F. 1990, ApJ, 365, 186

Grebel, E. K. 1999, in The Stellar Content of Local Group Galaxies, ed. P. Whitelock, & R. Cannon, IAU Symp., 192, 17

Groenewegen, M. A. T. 1999, in Asymptotic Giant Branch Stars, ed. T. Le Bertre, A. Lebre, & C. Waelkens, IAU Symp., 191, 535
Groenewegen, M. A. T., & Oudmaijer, R. D. 2000, A&A, 356, 849
Habing, H. J. 1996, A&AR, 7, 97
Iben, I. Jr., & Renzini, A. 1983, ARA&A, 21, 271
Lançon, A. 1999, in Asymptotic Giant Branch Stars, ed. T. Le Bertre, A. Lebre, & C. Waelkens, IAU Symp., 191, 579
Landolt, A. U. 1992, AJ, 104, 340
Palmer, L. G., & Wing, R. F. 1982, AJ, 87, 1739
Pickles, A. J. 1998, PASP, 110, 863
Richer, H. B. 1981, ApJ, 243, 744
Richer, H. B., Pritchet, C. J., & Crabtree, D. R. 1985, ApJ, 298, 240
Richer, H. B. 1989, in Evolution of Peculiar Red Giants, ed. H. R. Johnson, & B. Zuckerman, IAU Colloqu., 106, 35
Schultheis, M. 1998, Ph.D. Thesis, Univ. of Vienna
Stetson, P. B. 1987, PASP, 99, 191
Vassiliadis, E., & Wood, P. R. 1993, ApJS, 413, 641
Westerlund, B. E., Olander, N., Richer, H. B., & Crabtree, D. R. 1978, A&AS, 31, 61
Westerlund, B. E. 1979, ESO Messenger, 19, 7
Willson, L. A. 1988, Proc. Pulsation and Mass Loss in Stars, ed. R. Stalio, & L. A. Willson (Kluwer Academic Publishers), 285
Wing, R. F. 1971, in Proceedings of the Conference on Late-Tye Stars, ed. G. W. Lockwood, & H. M. Dyck, KPNO Contr. No. 554, 145
Wing, R. F., & Stock, J. 1973, ApJ, 186, 979
Zijlstra, A. A. 1999, in Asymptotic Giant Branch Stars, ed. T. Le Bertre, A. Lebre, & C. Waelkens, IAU Symp., 191, 551